CFD Modelling and Comparison among Different Configurations of Parallel Plates Iron Electrowinning Cells

Mónica Serna[1]

[1] Labein-Tecnalia, Derio, Spain

mserna@labein.es

Within the ULCOS project, a pilot cell for iron electrowinning is being designed. Electrical energy is used to transform iron ore particles (hematite) suspended in a sodium hydroxide solution into iron metal and oxygen. The work developed by Labein-Tecnalia is focused on the study of the fluid flow for different electrolytic cell configurations to get knowledge of the interaction between the oxygen bubbles generated during the process and the electrolyte flow. The numerical algorithm used is the finite volume used in the commercial Computational Fluid Dynamics code FLUENT. The work developed is focused on vertical and horizontal parallel plates configurations, to analyze the removal of oxygen bubbles from the gap between anode and cathode, and the access of iron ore particles to the cathode.

A user subroutine has been developed for the CFD code to compute the mass flow rate of oxygen bubbles generated at the anode, as a function of the local current density. A methodology has been developed to analyze the accessibility of the iron ore particles to the cathode.

The knowledge obtained from this work has helped for the design of the pilot cell within the ULCOS project.

Introduction

Results CFD simulations run for different designs of iron electrowinning cells are presented here. The cases analyzed are focused on vertical and horizontal parallel plates cells.

The electrolyte is a 50% sodium hydroxide solution, with iron ore particles of hematite. In simulations it has been considered a suspension of 1kg Fe_2O_3 + 1 kg of NaOH + 1 kg of H_2O, which density has been determined according to the volume weighted mixing law of CFD code:

$$\rho = \frac{1}{\sum_i \frac{Y_i}{\rho_i}}$$

where Y_i is the mass fraction and ρ_i is the density of the species *i*.

The oxygen bubbles generated at the anode due to the electrolytic reaction have been taken into account in the simulations by means of the Discrete Phase Model (DPM) of the CFD code, and they are assumed to be spherical and rigid.

Oxygen bubbles trajectories are the result of the force balance over them: drag forces of the fluid and gravitational forces. The turbulence effect is considered on bubbles movement (random walk model). Instantaneous fluid velocity, which dictates the bubble trajectory, is function of local turbulence and is updated every “eddy life time”. The following equations solve bubbles trajectories:

$$u_{pi} = \frac{dx_{pi}}{dt}$$

$$\frac{du_{pi}}{dt} = \frac{3}{4}\frac{\mu C_d \,\mathrm{Re}_p}{\rho_p d_p^2}\left(u_{pi} - u_i\right) + g\frac{\left(\rho_p - \rho\right)}{\rho_p} + a_{others}$$

$$u_i = \overline{u_i} + u_i'$$

$$u_i' = \zeta\sqrt{\overline{u_i}^2} \Leftrightarrow u_i' = \zeta\sqrt{\frac{2k}{3}}$$

where u_p is the particle velocity, μ is the molecular viscosity of the fluid, ρ_p is the particle density, p is the fluid density, C_d is the drag coefficient, Re is the Reynolds number, g is the gravity, d_p is the particle diameter, u_i is the instantaneous fluid velocity, $\overline{u_i}$ is the mean fluid velocity, u_i' is the fluctuating velocity, ζ is the turbulent kinetic energy.

The mass flow rate of oxygen bubbles has been determined according to Faraday’s Law:

$$q = Mj_n/(nF)$$

which determinates the local rate of produced gas by the electrochemical reaction, in the case of no back reaction (efficiency =100%). *q* is the gas phase local mass flow rate, j_n the current density normal to boundary, *n* is the charge number, *F* is the Faraday constant and *M* is the molar weight for oxygen bubbles. The charge number is determined by the electrolysis reaction equation of the hematite:

Cathode reaction:

$$2Fe_2O_3 + 6H_2O + 12e^- \rightarrow 4Fe + 12OH^-$$

Anode reaction:

$$12OH^- \rightarrow 12e^- + 3O_2 + 6H_2O$$

Overall reaction:

$$2Fe_2O_3 \rightarrow 4Fe + 3O_2$$

A user subroutine compiled with C has been developed to determine the mass flow rate of oxygen bubbles generated at the anode surface.

The main assumptions considered in the simulations are:

- Cell voltage: 0.067 V
- Distance between electrodes: 10 mm
- Temperature of the electrolyte: 110ºC
- Electrolyte density:1380 kg/m^3
- Iron ore density: 5250 kg/m^3
- Suspension density: 1830 kg/m^3
- Oxygen bubbles density: 1kg/m^3
- Suspension's electrical conductivity: 150S/m
- Viscosity of suspension: 0.0025 Pa·s

Regarding the cell voltage, it should be mentioned that thermodynamic effects and kinetic overpotentials are not considered in simulations.

The following hypotheses have been considered:

- Constant electrical potential at each electrode
  - Anode 0.067 V
  - Cathode 0 V
- Oxygen bubbles of 1 mm of diameter injected at the anode by means of a Discrete Phase Model (DPM) according to Faraday's Law (not considered coalescence effects)
- Current density is solved in CFD by means of a User Defined Scalar Function:

$$j = \kappa \cdot E = -\kappa \cdot grad\phi$$

where j is the current density in A/m^2, k is the electrical conductivity in S/m and ϕ is the electrical potential in Volts.

In simulations it is not considered the deposition of iron metal onto the cathode. The results are focused on analyzing the oxygen bubbles concentration and the accessibility of the iron ore particles to the cathode for different configurations.

Vertical Cell

The oxygen gas produced at the anode should be directed out of the electrolyte in order to not come in contact with the cathode, and not increase the resistance of the electrolyte.

To minimize the contact between the oxygen bubbles and the cathode several anodes shapes have been analysed for the vertical cell configuration.

The simulations are 2D and an electrodes' height of 1 meter has been considered.

In order to compare the different configurations analyzed, the same average velocity (0.2m/s) has been considered at the inlet of the gap between the anode and the cathode.

In Figure 1 it is shown one of the geometries, where a flat plate anode has been considered:

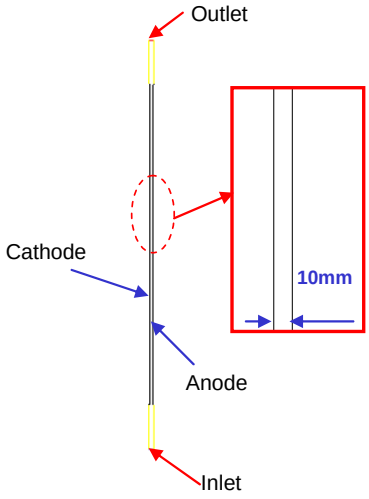

Figure 1. Geometry of the flat plate anode (electrode's height 1 m)

The oxygen bubbles generated at the anode accelerate the fluid as they rise, due to buoyancy. This phenomenon can be observed in Figure 2, where a uniform velocities profile is observed in the lower part of the gap anode-cathode, and higher velocities are achieved near the anode in the upper part of the gap.

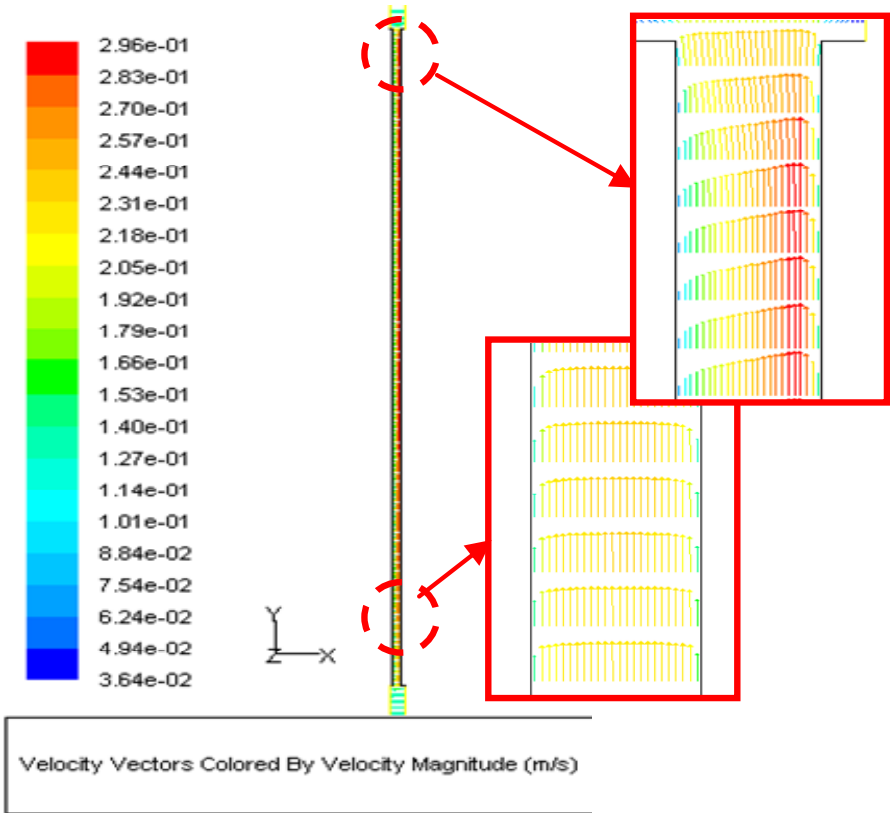

Figure 2. Velocity Vectors for the flat plate anode

The fluid acceleration due to oxygen bubbles increases turbulence in the upper part of the gap anode-cathode, as can be observed in Figure 3, which represents the contours of turbulence intensity, that is, the relation between fluctuating (u') and average (u_{avg}) velocities:

$$I_{turb} = \frac{u'}{u_{avg}}$$

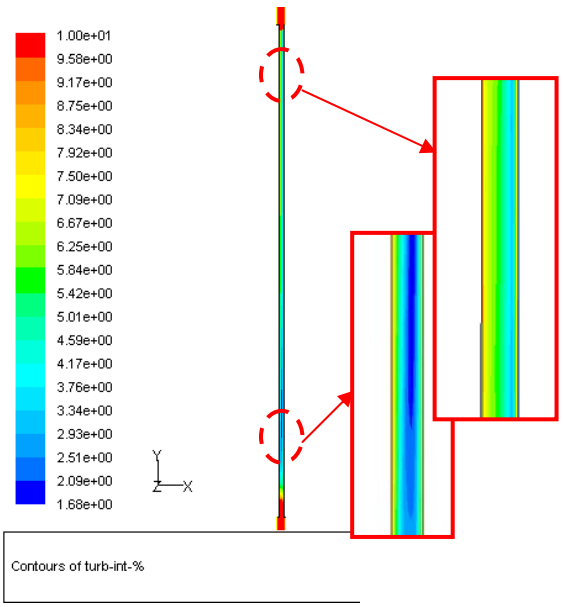

Figure 3. Turbulence intensity for flat plate anode configuration

Due to turbulence, oxygen bubbles can contact the cathode while rising, as can be observed in the trajectories of the bubbles depicted in Figure 4.

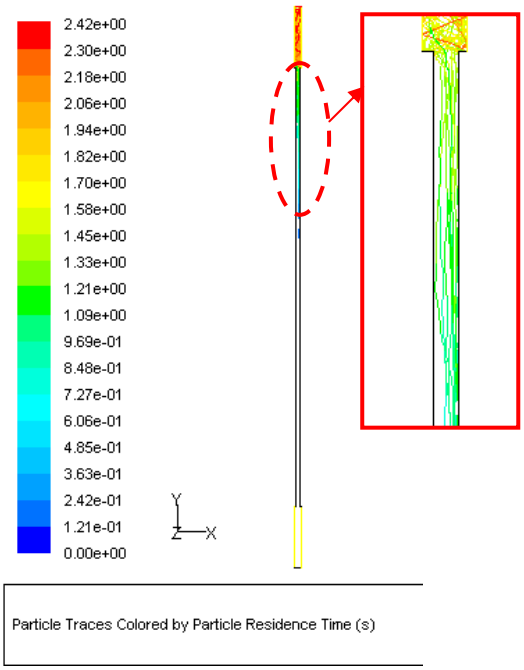

Figure 4. Oxygen bubbles trajectories

For the flat plate anode it has also been analyzed the influenced of the oxygen bubbles in current density along the cathode. By means of a custom function compiled with C, the influence of void fraction in

electrolyte conductivity has been determined according to Bruggeman's relation:

$$\kappa = \kappa_0 (1-\varepsilon)^{3/2}$$

where κ is the electrical conductivity, κ_0 stands for the electrical conductivity of the pure electrolyte (150 S/m in our case), and ε is the local void fraction.

The following figure (Figure 5) shows the current density profile on cathode vs. cathode's height. The normalized standard deviation determined is 1%, so the influence of oxygen bubbles on current density is small.

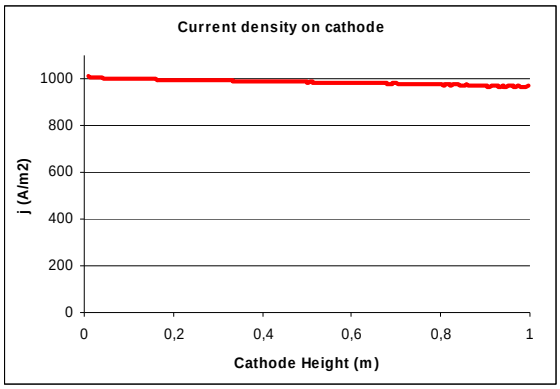

Figure 5. Current density on cathode for flat plate anode configuration

It has also been analysed a geometry in which venetian curtain like anode is used, made of several slats inclined. Two geometries have been considered, for two different tilt angles of the slats, 50 and 60 degrees. In both configurations there are 100 slats along the electrode's height. The geometries have been named as "sloped anode 50º" and "sloped anode 60º" (Figure 6).

The symmetry boundary condition implies that next to the anode there is another anode. The idea of these configurations was to direct the oxygen bubbles generated at the anode between the slats, avoiding their contact with the cathode.

Oxygen bubbles generation depends on current density normal to anode (according to Faraday's Law), which is not uniform along the electrode, and has a maximum at the tip of the slat closer to the cathode (Figure 8), therefore most of the bubbles are generated at that point. Due to the recirculations between the slats depicted in Figure 7, oxygen bubbles do not have a preferential path upwards between the slats. Therefore, they can rise on both sides of the anode (Figure 9), that is, between the slats or through the gap cathode-anode.

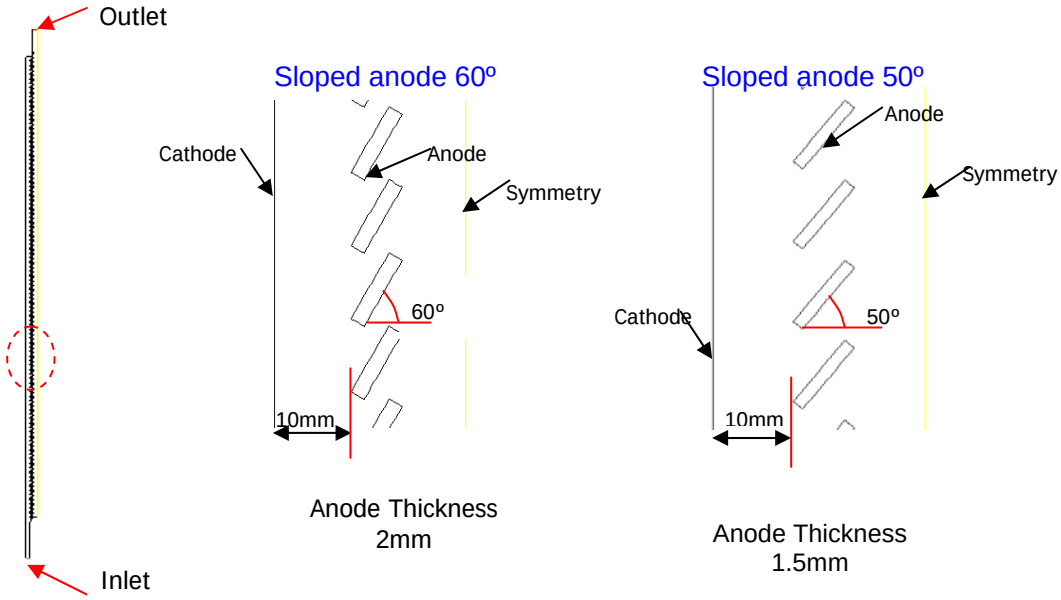

Figure 6. Geometry of the sloped anodes configurations

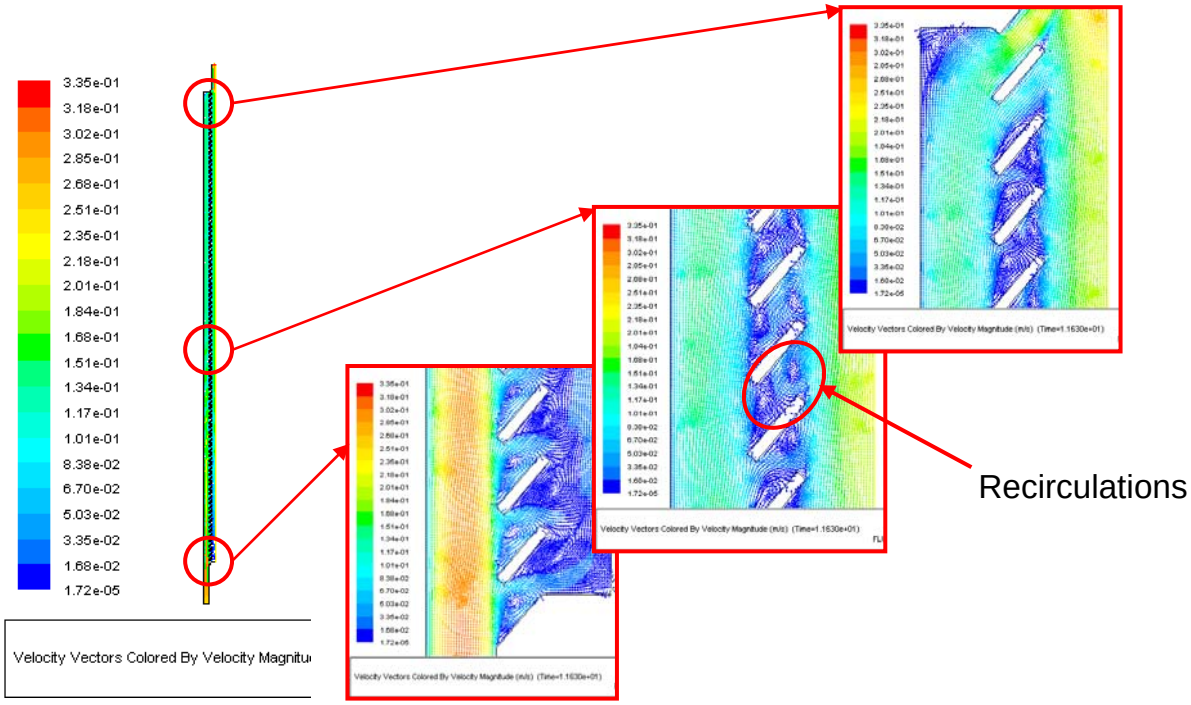

Figure7. Velocity Vectors for the sloped anode 50º geometry

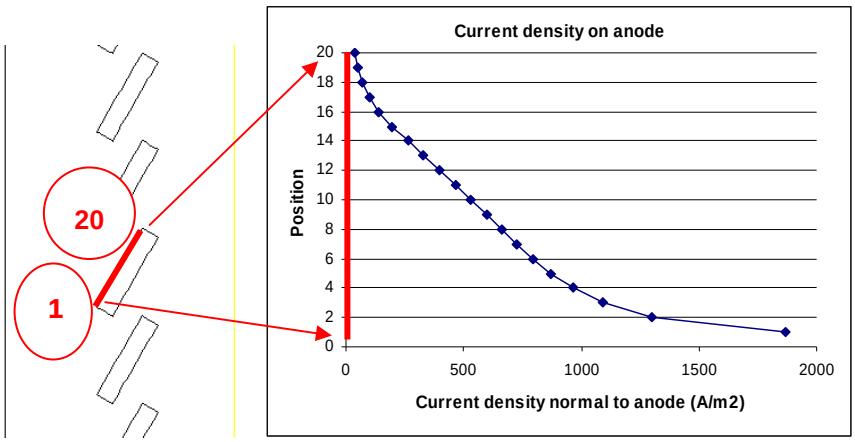

Figure 8. Current density normal to anode for sloped configuration

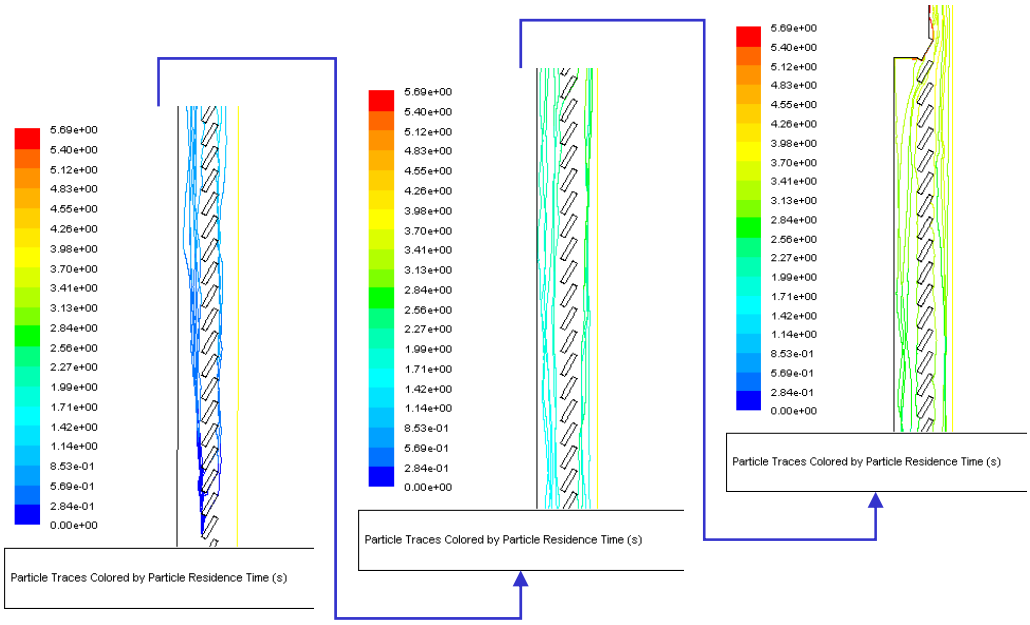

Figure 9. Trajectories of O2 bubbles generated at the tip of the anode closer to the cathode (sloped anode 60º configuration)

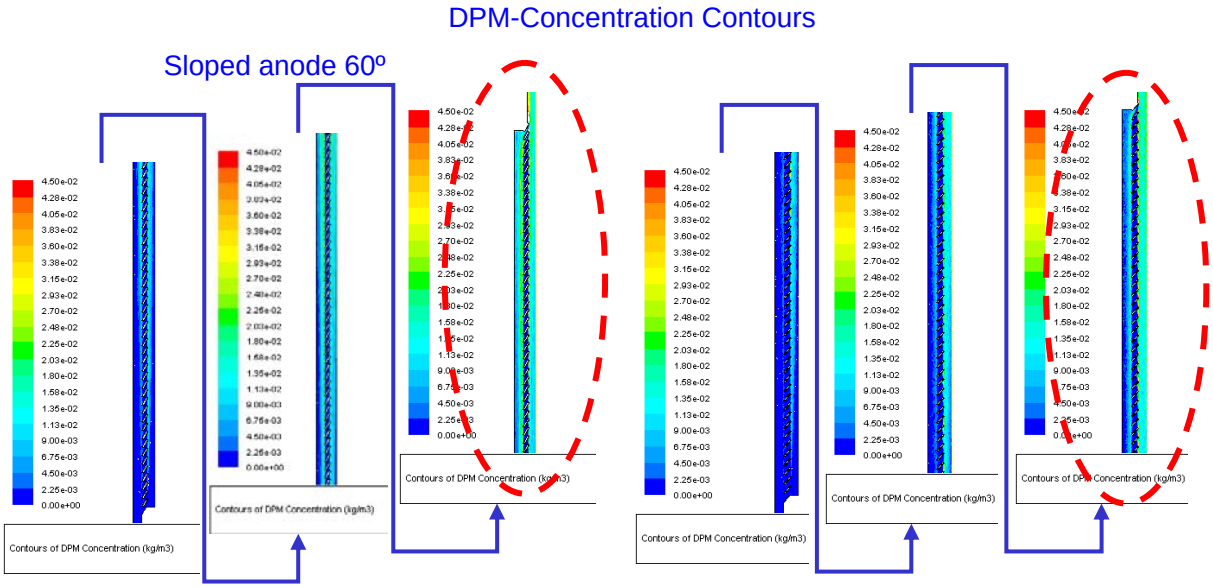

Figure 10. Oxygen bubbles concentration

Analyzing the oxygen bubbles concentration in the gap anode-cathode, it is observed that there are fewer bubbles for the configuration of the sloped anode 50º. This fact is better appreciated in the upper part of the cell (Figure 10).

The comparison between the geometries in terms of oxygen bubbles concentration on the cathode, shows lower concentrations values for the 50º sloped anode geometry (Figure 11) than for the flat plate anode and the 60º sloped anode geometries.

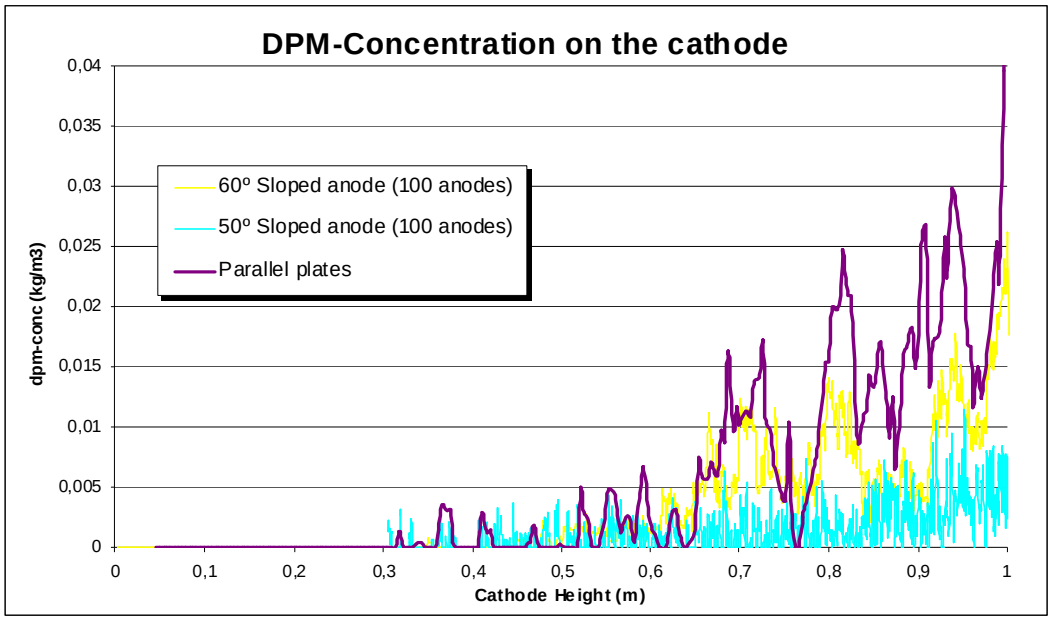

Figure 11. DPM-concentration (O_2) on cathode

In order to obtain a uniform iron deposit on the cathode it is interesting to study the accessibility of the iron ore particles to the cathode. The methodology developed for this purpose is described below:

- During 1 second, particles of 10 μm are injected through the inlet.
- It is determined the number of particles that contact the cathode at each height interval (assuming that each particle that contacts the cathode is trapped). For this purpose, the cathode height has been divided in equal intervals, and the number of particles that contact the cathode at each height's interval has been determined to obtain the particles' percentage dividing the number of particles by the total number of particles injected.

$$\%particles = \frac{particles_{interval}}{particles_{injected}}$$

In simulations the injection is not continuous, therefore the number of particles decreases with cathode's height as they are trapped, so higher percentage of particles are obtained in the lower zone.

The results obtained are summarized in the following figure (Figure 12). For the flat plate anode, all the particles injected have to pass through the gap between anode and cathode, therefore a higher percentage of particles are obtained.

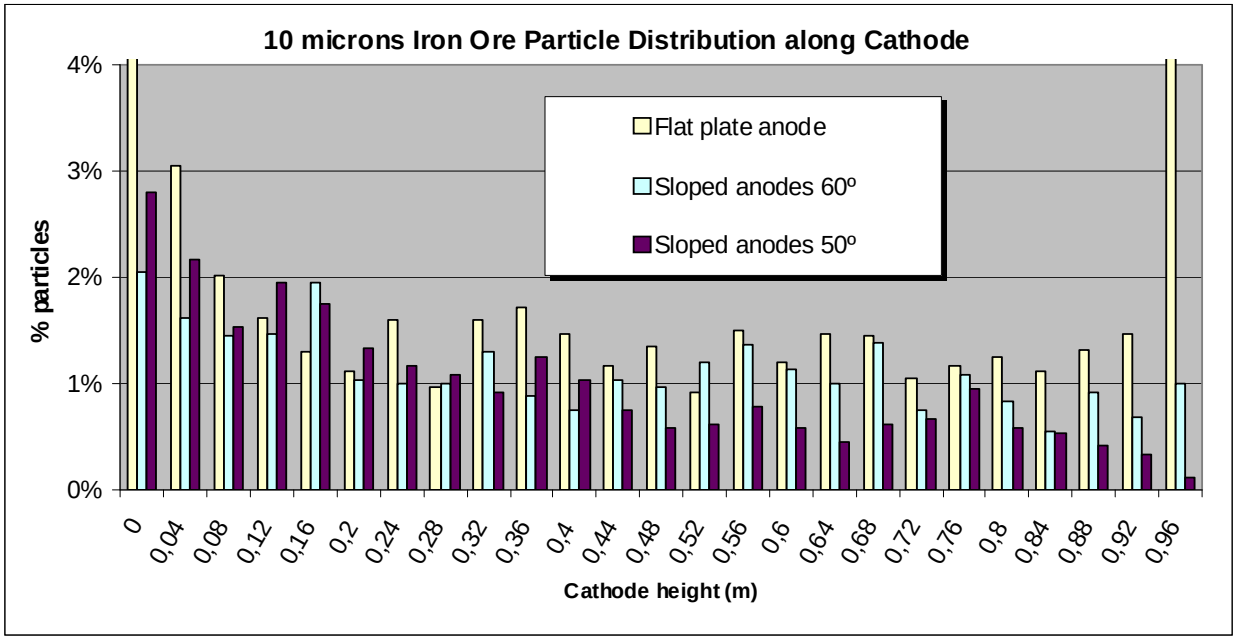

Figure 12. Accessibility of iron ore particles to the cathode

From Figure 11 it can be concluded that there is a supply of iron ore particles all over the cathode for the geometries analyzed. In order to compare the results obtained, the normalized standard deviation of the contact frequency of the iron ore particles with the cathode has been determined, and it is depicted in Figure 13. A more uniform accessibility is obtained for the flat plate anode and for the 60º sloped anode geometries.

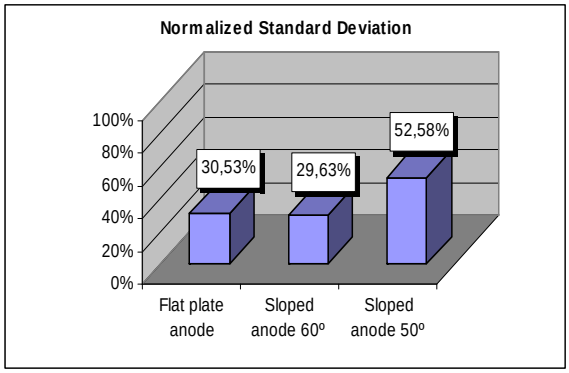

Figure 13. Normalized standard deviation of accessibility of iron ore particles to the cathode

Horizontal Cell

3D simulations have been carried out for the horizontal laboratory cell installed at LSGC-INPL (Nancy, France) facilities (Figure 14). The cell is composed of a top nickel anode oriented downward and a bottom graphite cathode oriented upward. Both electrodes have a reactive surface amounting to 21 cm^2. These electrodes are parallel facing each other. The cathode is in the bottom side of the chamber, and the anode in the upper side. Both of them are rectangles of 60mm x 35mm, which are located in a chamber of 96.3mm x 80mm. The gap between the electrodes is 10mm, and the diameter of the input and output pipes is 12mm.

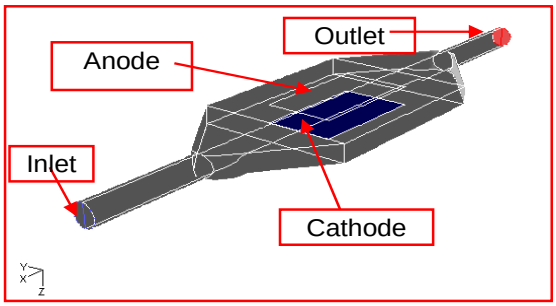

Figure 14. Geometry of the horizontal laboratory cell

Due to the symmetry of the horizontal cell, only half of the geometry has been considered in simulations. The results presented correspond to an electrolyte (1kg NaOH + 1kg H_2O + 1kg Fe_2O_3) flow rate of 350 l/h. The hypothesis and assumptions considered in simulations are the ones described in the introduction.

Analyzing the fluid flow inside the cell, it is observed that there is a preferential path of electrolyte straight ahead between inlet and outlet, and recirculations in the wide part of the cell chamber (Figure 15). In Figure 16 the velocities profile shown higher velocities in the central region with values close to 0.8 m/s, six times higher than the average velocity in that section (0.12 m/s).

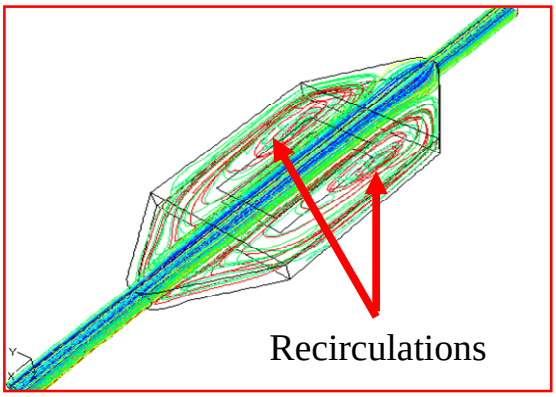

Figure 15. Electrolyte pathlines

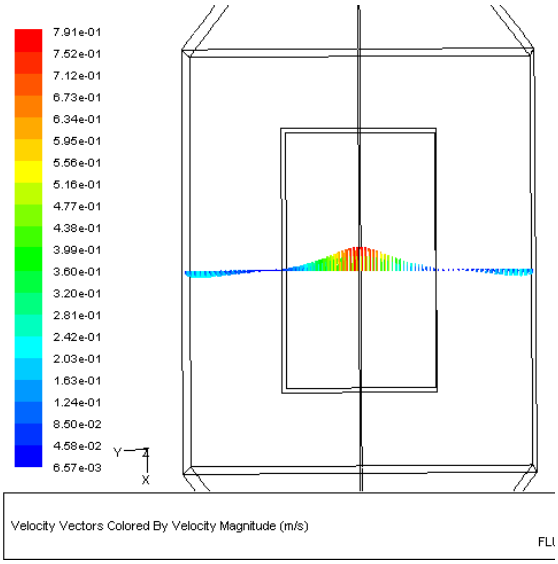

Figure 16. Velocity vectors in a transversal plane (top view)

The recirculations observed inside the cell, caused the accumulation in that regions of the oxygen bubbles (ρO_2=1kg/m^3) generated at the anode (Figure 17).

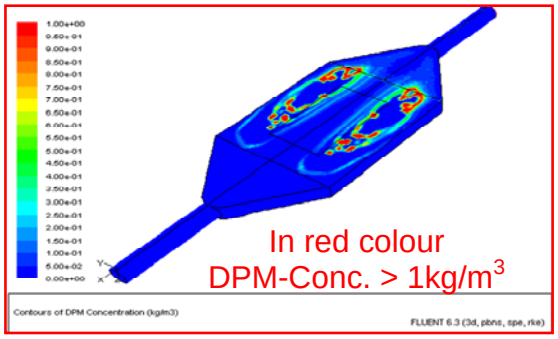

Figure 17. Contours of oxygen bubbles concentration (kg/m^3)

To analyze the accessibility of iron ore particles to the cathode, it has been followed the same methodology explained for the vertical cells:

- Particles of 10, 20 and 50 μm have been injected through the inlet during 1 second
- It is determined the number of particles that contact the cathode at each interval (assuming that each particle that contacts the cathode is trapped). For this purpose, the cathode has been divided in 200 subdivisions (see Figure 18), and the number of particles that contact the cathode at each subdivision has been determined to obtain the particles' percentage dividing the number of particles by the total number of particles injected:

$$\%particles = \frac{particles_{interval}}{particles_{injected}}$$

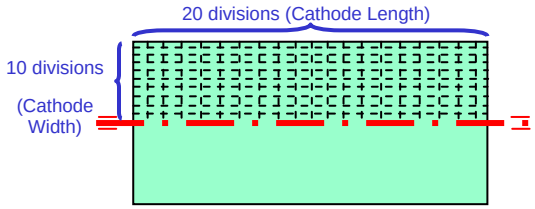

Figure 18. Cathode subdivisions (top view)

In simulations the injection is not continuous; therefore, the number of particles decreases as they are trapped, so higher percentage of particles are obtained near the inlet.

In Figure 19 it is depicted the percentage of particles trapped at each cathode subdivision when iron ore particles of 10 microns are injected. Higher percentage of particles are trapped in the central region because of the higher velocities of that zone. The supply of iron ore particles is not homogeneous all over the cathode, a normalized standard deviation of 66% has been obtained. Around 14% of the entering particles (the sum of the percentage at each cathode's subdivision) "touch" the cathode, the rest of them escape through the outlet. For 20 microns particles the normalized standard deviation is 63% and 15% of the entering particles reach the cathode.

When particles of 50 microns are injected, the accessibility of the iron ore particles to the cathode is more homogenous than in the cases of iron ore particles of 10 and 20 microns. The normalized standard deviation calculated is 55%, and 19% of the entering particles reach the cathode. In Figure 20 is depicted the distribution of the percentage of particles over the cathode.

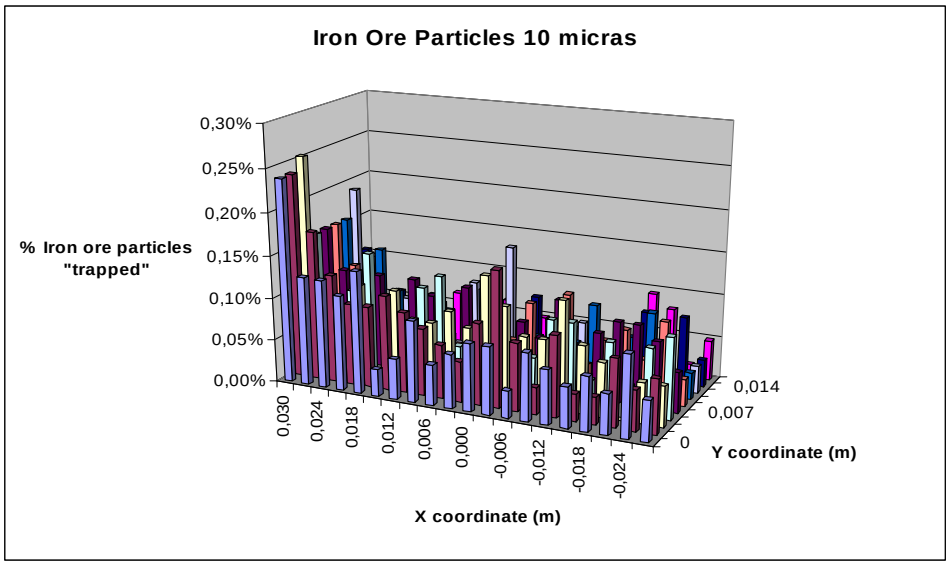

Figure 19. Percentage of particles of 10 μm "trapped" at each cathode subdivision

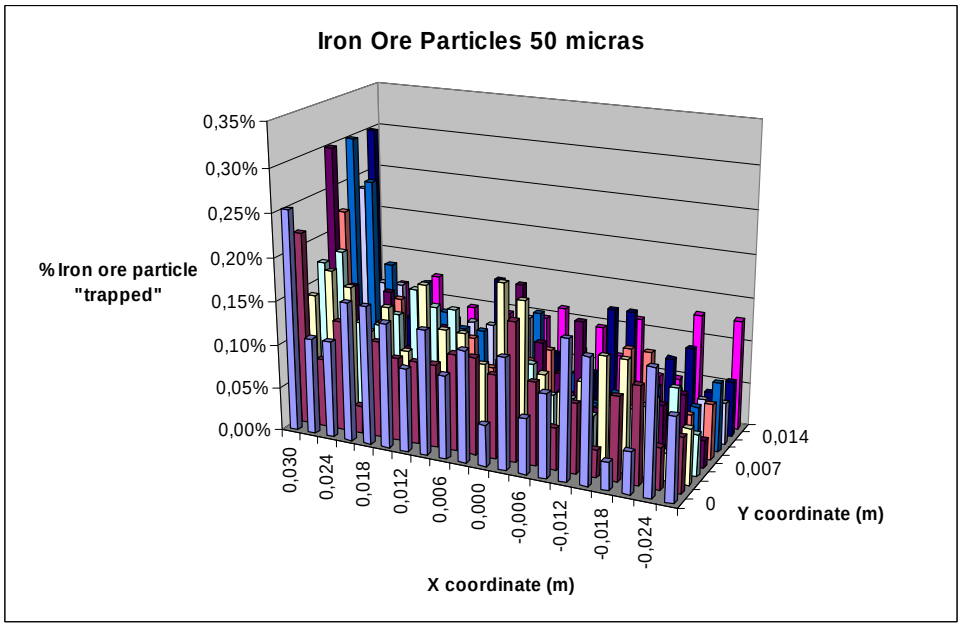

Figure 20. Percentage of particles of 50 μm "trapped" at each cathode subdivision

Conclusion

A computational study has been performed for different geometries of electrowinning cells and compare in terms of oxygen bubbles concentration and accessibility of iron ore particles to the cathode. Computations are performed with FLUENT and oxygen bubbles injection at the anode has been included by a custom function compiled with C, calculating the gas flow rate according to Faraday's law (first law of electrolysis). The bubbles are assumed to be spherical and rigid, and no coalescence effects are considered.

A methodology has been developed to analyze the accessibility of the iron ore particles to the cathode, by means of a punctual injection of particles through the inlet.

For the vertical cell configurations analyzed, regarding the oxygen gas concentration on the cathode the best option will be the "sloped anode 50 degree", although the "sloped anode 60°" configuration shows a better accessibility of the iron ore particles to the cathode.

For the geometry of the horizontal cell, the recirculations observed in the electrolyte flow caused the accumulation of oxygen bubbles. The accessibility of iron ore particles to the cathode has been analyzed for three different particles sizes (10μm, 20μm and 50 μm). The results obtained are

slightly better for the particle diameter of 50μm (lower normalized standard deviation and higher percentage of particles that reach the cathode).

The knowledge obtained from this work has helpful to design a new pilot cell built by ArcelorMittal. Further simulations will be carried out for this cell to validate the model with experimental data.

Acknowledgements

The present work is part of the ULCOS program, which operates with direct financing from its 48 partners, especially of its core members (Arcelor-Mittal, Corus, TKS, Riva, Voestalpine, LKAB, Saar-stahl, Dillinger Hütte, SSAB, Ruukki and Statoil), and has received grants from the European Commission under the 6th Framework RTD program and the RFCS program[1].

References

[1] R. H. Perry, D. W. Green, "Perry's Chemical Engineers' Handbook", 7th edition, Mc Graw Hill, 1997

[2] F. Hine, "Electrode Processes and Electrochemical Engineering", Plenum Press, New York, 1977

[3] M. Philippe et al. "Modelling and calculation of the current density distribution evolution at vertical evolving electrodes", Electrochimica Acta 51, 2005 (1140 – 1156)

[1] Priority 3 of the 6th Framework Programme in the area of "Very low CO_2 Steel Processes", in co-ordination with the 2003 and 2004 calls of the Research Fund for Coal and Steel